Title: Agricultural expansion dominates climate changes in southeastern Amazonia: The overlooked non-GHG forcing

Authors: Divino V. Silvério, Paulo M. Brando, Marcia N. Macedo, Pieter S.A. Beck, Mercedes Bustamante, Michael T. Coe

Study area - Our study area is the upper Xingu basin in Mato Grosso, Brazil, a 176,892 km² area in southeast Amazonia that is dominated by transitional forests. The region encompasses the Xingu Indigenous Park and several adjacent indigenous reserves, which form a large (34,503 km²) mosaic of protected areas, hereafter referred to as the XIP. The area outside the parks is composed of private properties, many of which have been deforested and converted to croplands or pastures (Schwartzman *et al* 2013). In 2001 61% of the study area was forest, 24.5% was pasture and 1.2% was croplands, mostly soybeans. The remaining 13.3% of the area was occupied by cerrado, a native savanna (non-forest vegetation). By 2010, the forested area had decreased to 49% and the extent of pasture and cropland had increased to 31% and 6% of the total area, respectively. Almost all of the forest loss during this period occurred on private lands outside the XIP (Macedo et al., 2012). At the same time, 4,962 km² of pasturelands were converted to croplands (2.8% of the upper Xingu basin).

S2. Net radiation estimation

Net radiation (R_{net}) at the land surface can be expressed as

$$R_{net} = R_S^{\downarrow}(1 - albedo) + R_l^{\downarrow} - R_l^{\uparrow}$$

Where Rs is downward shortwave radiation; *albedo* is the reflection coefficient of the shortwave radiation; and Rl and Rl are the downward and upward longwave radiation fluxes respectively. We estimated daily average R_{net} under all sky conditions using MODIS and weather station data, according to previously published methods for calculating R_{net} based on remote sensing products (Bisht and Bras 2010, Bisht et al., 2005, Ryu et al., 2008). We followed five steps (a-e) to calculate R_{net} (Fig. S1).

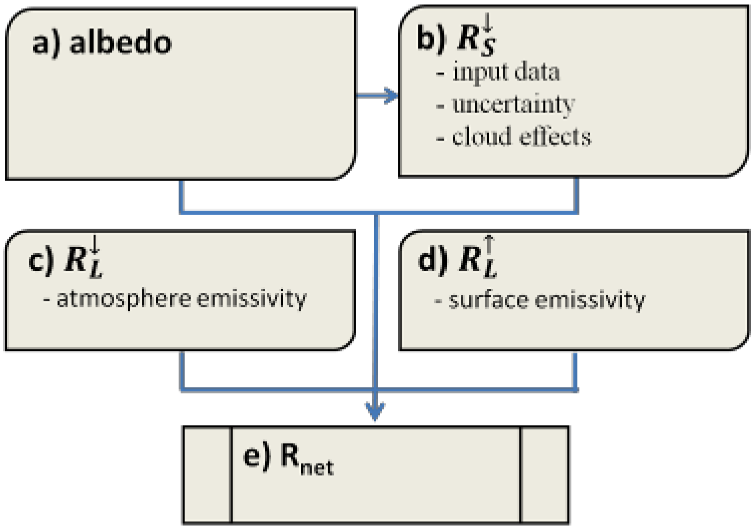

Fig. S1. Diagram of steps to calculate net radiation based on MODIS and weather station data.

a) Albedo –We calculated actual albedo using the broadband black-sky and white-sky (0.25 – 4.0µm) albedo layers from the 500 m MODIS albedo product (MOD43A3, collection 005), as in Eq. 2 (Schaaf *et al* 2002):

$$albedo = [1 - S(\theta, t)]\alpha_{bs} + S(\theta, t)\alpha_{ws}$$

where t is the atmospheric optical depth (AOD), S(omega, t) is the fraction of diffuse light, alpha bs is the black-sky albedo, alpha ws is the white-sky albedo. We retreived S(omega, t) from the look-up table available in the MOD43 software (Schaaf *et al* 2002). We calculated the actual albedo at local noon and we retrieved AOD from MOD08 (Hubanks et al., 2014) (we assumed that AOD was homogeneous in our study area).

b) Downward shortwave radiation (Rs) - We estimated Rs daily for clear sky days as described in Bird and Hulstrom (1981) and implemented by the *insolation* function in the *insol* R package (Corripio 2014). Based on solar position algorithms, the model computes direct and diffuse solar irradiance perpendicular to the beam, for a given zenith angle (one-hour intervals from sunrise to sunset), Julian Day (every 8 days), altitude, and atmospheric condition (Corripio 2003, Reda and Andreas 2004, Bird and Hulstrom 1981).

The input data to calculate Rs was altitude (derived from a 1 km DEM;

http://www.worldclim.org), air temperature, relative humidity (RH), albedo of the surrounding terrain, ozone thickness (OZ) and atmospheric optical depth (AOD). The air temperature and RH were estimated by kriging data from 12 weather stations belonging to the Brazilian National Meteorological Institute (INMET) (INMET 2012) (Table S1). Albedo was calculated based on MOD43A2 as explained in step (a). We used OZ (at 550 nm) and AOD from the 8-day MODIS atmospheric product (MOD08E3) (Hubanks et al., 2014). We assumed that OZ and AOD were homogeneous in a 1º grid. AOD was used to calculate horizontal visibility in km (as in Eq. 64 of Román *et al* (2010)).

We calculated the effect of clouds on Rs using Eq. 3 (Bisht and Bras 2010):

$$R_S^{\downarrow cloudy} = R_S^{\downarrow} [(1 - f_c) + f_c e^{-t_c/cos(\theta)}]$$

where Rs is estimated shortwave radiation for clear sky days, fc is cloud fraction (retrieved from MOD08E3 (Hubanks et al., 2014)), tc is cloud optical thickness (MOD08E3), and omega is the solar zenith angle (MOD08E3).

c) Downward longwave radiation (Rl) – We calculated Rl for all sky condition by using Eq. 4 (Bisht and Bras 2010):

$$R_L^{\downarrow} = \sigma \varepsilon_a T_a^4 + \sigma(1-\varepsilon_a)\varepsilon_c T_c^4$$

Where σ is the Stefan-Boltzmann constant (5.67 X 10^{-8} W m^{-2} K^{-4}), is atmosphere emissivity, T_a is air temperature (from INMET weather stations), is cloud emissivity (MOD08E3), and T_c is cloud temperature (MOD08E3). To estimate epsilon a we first estimated the dew point temperature based on relative humidity (as in Eq. 64 of Lawrence (2005)), then calculated near surface pressure (Rogers and Yau 1989), and finally calculated epsilon a using the scheme proposed by Prata (1996).

To estimate epsilon awe first computed the near-surface vapor pressure (e sub zero) as in Eq. 5 (Rogers and Yau 1989), where L_v is the latent heat of vaporization (2.5x10^6 [J kg^{-1}]), R_v is the gas constant for water vapor (461 [J kg^{-1}]) and T_d is the dewpoint temperature, computed based on relative humidity (Lawrence 2005). Then we computed epsilon a using the scheme proposed in Prata (1996):

$$e_0 = 6.11\, exp\left[\frac{L_V}{R_V}\left(\frac{1}{273.15} - \frac{1}{T_d}\right)\right]$$

$$\varepsilon_a = 1 - (1 + \xi)\exp\left(-\sqrt{(1.2 + 3\xi)}\right)$$

(d) Upward longwave radiation (R_L) – We calculated (R_L) using land surface temperature and surface emissivity (Ryu et al., 2008):

$$R_L^{\uparrow} = \sigma \varepsilon_s T_s^4 + (1-\varepsilon_s) R_L^{\downarrow}$$

Where σ is the Stefan-Boltzmann constant (5.67 X 10^{-8} W m^{-2} K^{-4}), ε_S is surface emissivity, T_s is surface temperature in Kelvin (MOD11A2), and R_l is downward longwave radiation (Bisht and Bras 2010).

The surface emissivity was calculated as:

$$\varepsilon_S = 0.273 + 1.778\ \varepsilon_{31} - 1.807\ \varepsilon_{s31}\ \varepsilon_{32} - 1.037\ \varepsilon_{32} + 1774\ \varepsilon^2_{32}$$

where ε31 and ε32 are the emissivity in bands 31 and 32 of MOD11A2 product. These bands are in the thermal infrared regions.

Net Radiation (R net)-Daily average Rnet was estimated under all sky conditions

S4. Data uncertainty

Our estimated shortwave radiation for clear sky days showed good agreement to observed data from a nearby INMET (INMET 2012) weather station (INMETA916, located at -12.62°S, -52.22°W, in Querência Mato Grosso) (Fig. S2).

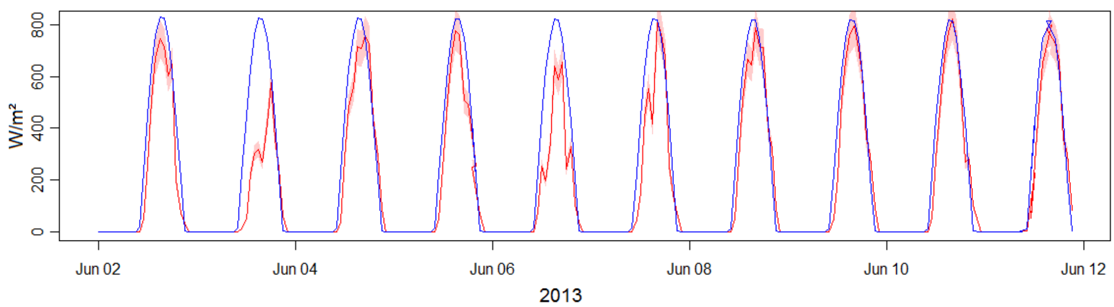

Fig. S2. Comparison of simulated global short wave radiation for clear sky days (blue line) and observed solar radiation from INMET weather station in Querência (red line), Mato Grosso (-12.62°S -52.22°W).

Net radiation (Rnet) - To validate our Rnet estimates, we used measurements from a net radiometer installed on a tower in Sinop, Mato Grosso (-13.06°S, -52.38°W; Beija-flor Project: www.lba.cptec.inpe.br/beija-flor). The daily mean of these in situ Rnet measurements was 11.45 (SD±2.06) MJ m^2 day^{-1} between 2000 and 2002, compared to

11.37 (SD±1.77) MJ m^2 day^{-1} in the MODIS-based estimates for the same location and period. We also averaged the in situ measurements every 8 days to match the temporal resolution of the MODIS data. A comparison of the two datasets indicates that the MODIS-based estimates adequately capture the actual Rnet in terms of magnitude (root mean square errors = 1.15 MJ m^2 day^{-1}; 10%; Fig. S5) and seasonality (Fig. S4).

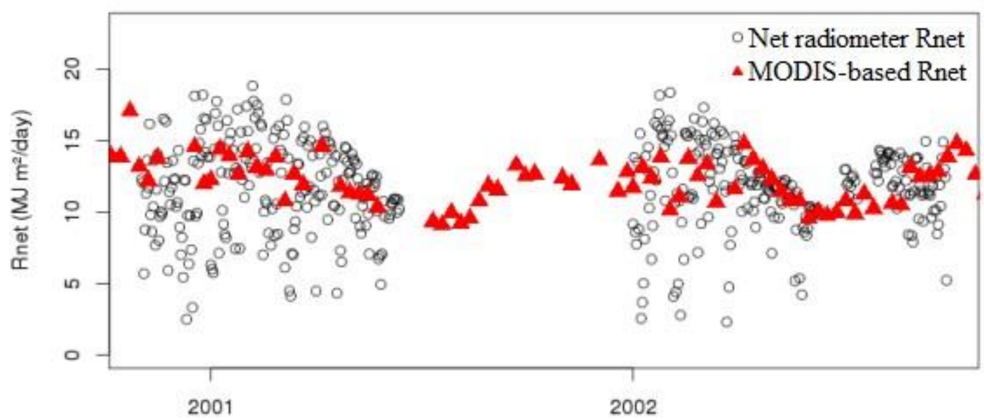

Fig. S4. Comparison of MODIS-based estimates of Rnet (every 8 days) and daily measurement from a net radiometer on an eddy flux tower located in Sinop, Mato

Grosso.

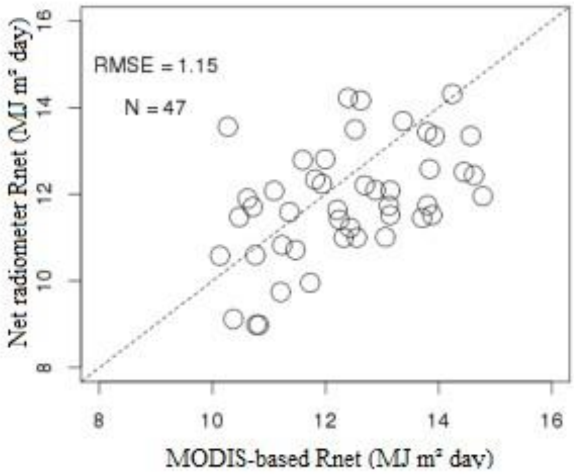

Fig. S5. Comparison of R_{net} measured with a net radiometer on an eddy flux tower in Sinop and MODIS-based R_{net} estimates. All data are shown as 8-day means. RMSE = Root Mean Square Error.

Table S4. Daily mean of albedo, net longwave, net shortwave and net radiation for the three land cover types analyzed in the upper Xingu basin (standard deviation in parenthesis).

Land cover	Albedo (reflectivity)	(MJ m^{-2} day^{-1})		
		Net longwave	Net shortwave	Net radiation
Forest	0.130 (0.002)	-2.65 (0.196)	15.29 (0.24)	12.64 (0.31)
Pasture	0.143 (0.003)	-3.93 (0.196)	15.15 (0.24)	11.22 (0.34)
Cropland	0.164 (0.003)	-4.25 (0.200)	14.68 (0.26)	10.43 (0.32)

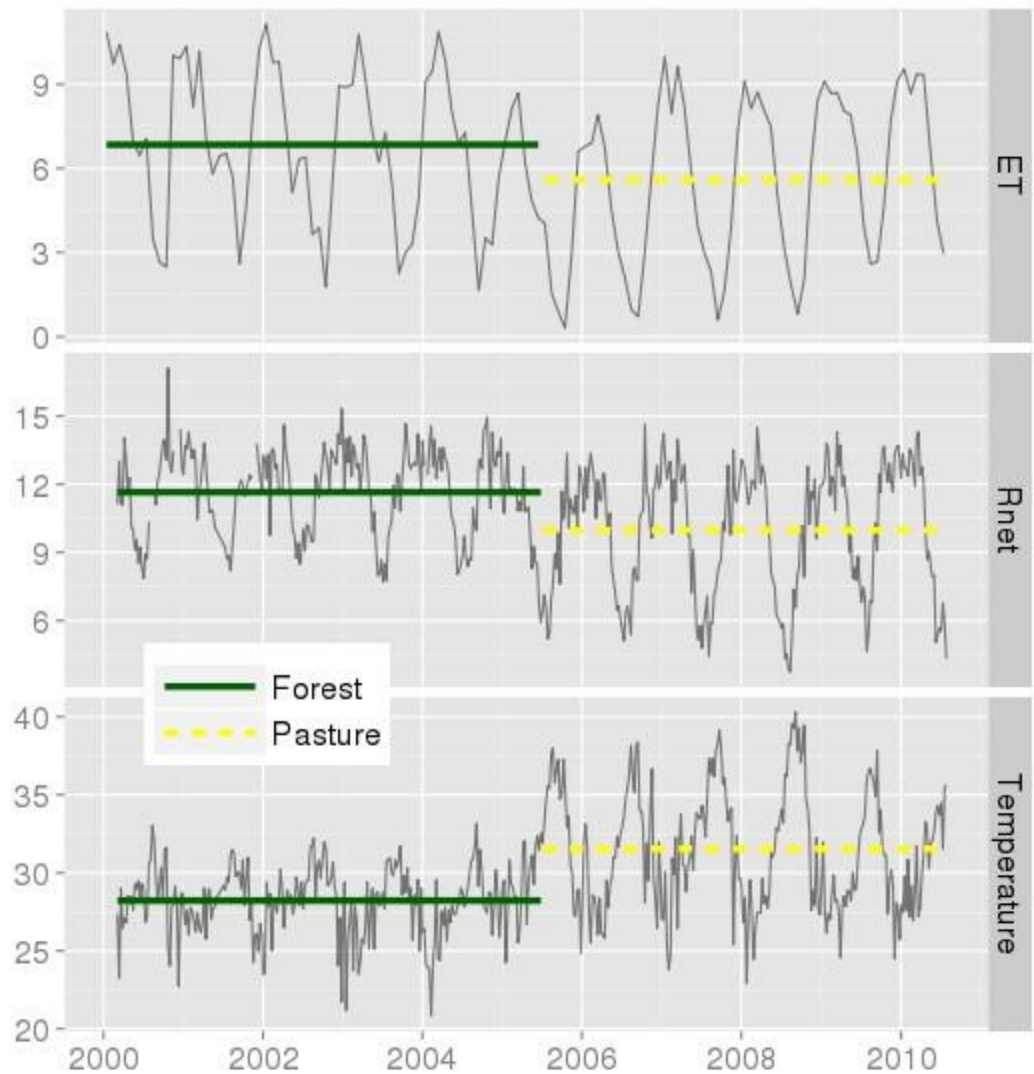

Fig. S7. Temporal pattern of evapotranspiration (ET, MJ m^{-2} day^{-1}), net radiation (R_{net}, MJ m^{-2} day^{-1}), and land surface temperature (°C) for three polygons experiencing a forest-to-pasture transitions in 2005 in the upper Xingu basin. Horizontal lines represent the average over the period when the area was covered by forest (solid line) or pasture (dashed line).

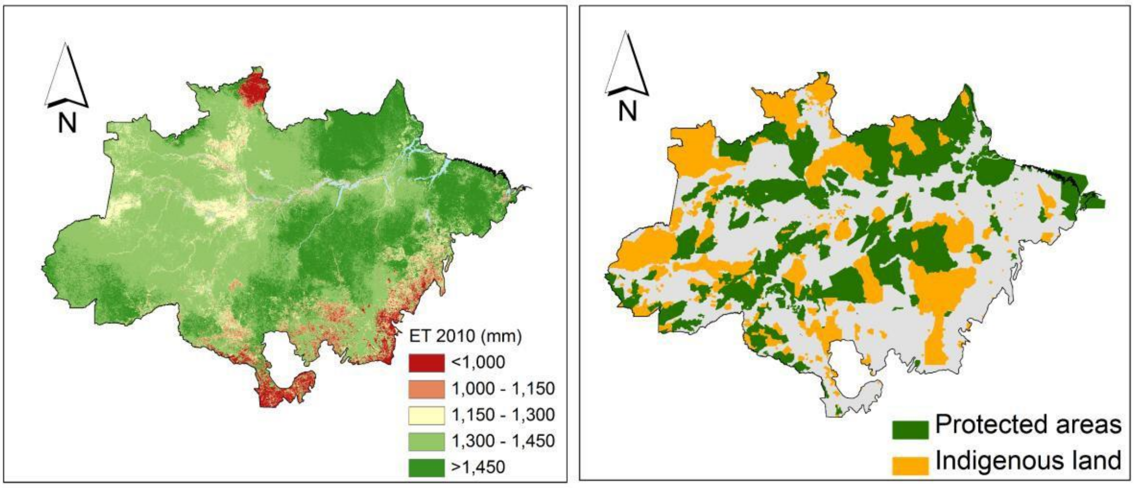

Fig. S8. Yearly mean of ET in 2010 from MOD16A3 (right panel) and protected areas and indigenous land in the Brazilian Amazon Biome (left panel).

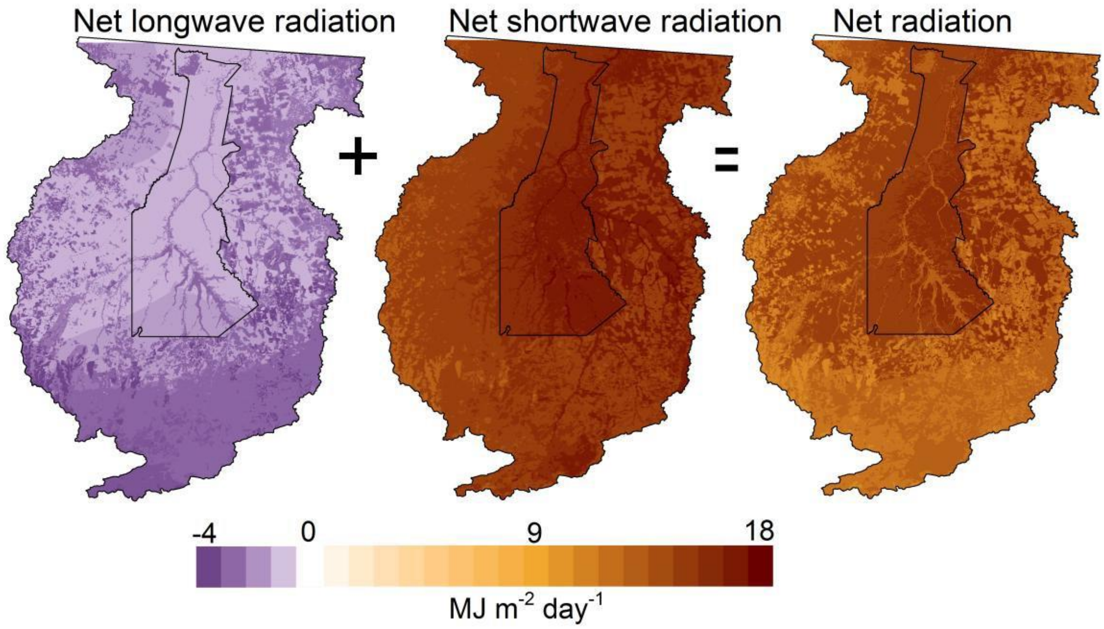

Fig. S9. Net shortwave radiation (incoming shortwave solar radiation minus the fraction reflected by the land surface), net longwave radiation (the difference between incoming and outgoing longwave radiative fluxes) and net radiation (net longwave plus net shortwave radiation) in 2010 for the upper Xingu basin in MJ m-^{2} day-1.

References

Bird R E and Hulstrom R L 1981 Review, evaluation, and improvement of direct irradiance models ASME 103 182–92.

Bisht G and Bras R L 2010 Estimation of net radiation from the MODIS data under all sky conditions: Southern Great Plains case study Remote Sens. Environ. 114 1522–34 .

Bisht G, Venturini V, Islam S and Jiang L 2005 Estimation of the net radiation using MODIS (Moderate Resolution Imaging Spectroradiometer) data for clear sky days Remote Sens. Environ. 97 52–67.

Corripio J G 2014 insol: Solar Radiation. R package version 1.1.1 http://cran.r – project.org/web/packages/insol/index

Corripio J G 2003 Vectorial algebra algorithms for calculating terrain parameters from DEMs and solar radiation modelling in mountainous terrain Int. J. Geogr. Inf. Sci. 17 1–23

Hijmans R J, van Etten J, Etten J van, Mattiuzzi M, Sumner M, Greenberg J A, Lamigueiro O P, Andrew Bevan, Racine E B and Shortridge A 2014 raster: Geographic analysis and modeling with raster data. R package version 2.2-31 http://cran.r – project.org/web/packages/raster/

Hubanks P A, Pincus R and Liang X 2014 MODIS Atmosphere: Eight-Day Global Product NASA http://modis – atmos.gsfc.nasa.gov/MOD08_E3/

INMET 2012 Monitoramento das estações meteorológicas convencionais MAPA - Inst. Nac. Meteorol. http://www.inmet.gov.br/html/rede_obs.php

Lawrence M G 2005 The Relationship between Relative Humidity and the Dewpoint Temperature in Moist Air: A Simple Conversion and Applications Bull. Am. Meteorol. Soc. 86 225–33

Loarie S R, Lobell D B, Asner G P, Mu Q and Field C B 2011 Direct impacts on local climate of sugar-cane expansion in Brazil Nat. Clim. Chang. 1 1–24.

Macedo M N, DeFries R S, Morton D C, Stickler C M, Galford G L and Shimabukuro Y E 2012 Decoupling of deforestation and soy production in the southern Amazon during the late 2000s Proc. Natl. Acad. Sci. 109 1341–6.

Mu Q, Zhao M and Running S W 2011 Improvements to a MODIS global terrestrial evapotranspiration algorithm Remote Sens. Environ. 115 1781–800.

Prata A J 1996 A new long-wave formula for estimating downward clear-sky radiation at the surface Q. J. R. Meteorol. Soc. 122 1127–51.

Reda I and Andreas A 2004 Solar position algorithm for solar radiation applications Sol. Energy 76 577–89.

Rogers R R and Yau M K 1989 A short course in cloud physics (Butterworth Heinemann)

Román M O, Schaaf C B, Lewis P, Gao F, Anderson G P, Privette J L, Strahler A H, Woodcock C E and Barnsley M 2010 Assessing the coupling between surface albedo derived from MODIS and the fraction of diffuse skylight over spatially-characterized landscapes Remote Sens. Environ. 114 738–60

Ruhoff A L, Aragão L E, Collischonn W, Rocha H R da, Yadvinder Malhi, Mu Q and Running S W 2013 Modelagem da evapotranspiração em áreas de floresta tropical amazônica Simpósio Brasileiro de Sensoriamento Remoto (Foz do Iguaçu) pp 1–8

Ryu Y, Kang S, Moon S-K and Kim J 2008 Evaluation of land surface radiation balance derived from moderate resolution imaging spectroradiometer (MODIS) over complex terrain and heterogeneous landscape on clear sky days Agric. For. Meteorol. 148 1538–52

Schaaf C B, Gao F, Strahler A H, Lucht W, Li X, Tsang T, Strugnell N C, Zhang X, Jin Y, Muller J-P, Lewis P, Barnsley M, Hobson P, Disney M, Roberts G, Dunderdale M, Doll C, D'Entremont R P, Hu B, Liang S, Privette J L and Roy D 2002 First operational BRDF, albedo nadir reflectance products from MODIS Remote Sens. Environ. 83 135–48

Schwartzman S, Boas A V, Ono K Y, Fonseca M G, Doblas J, Zimmerman B, Junqueira P, Jerozolimski A, Salazar M, Junqueira R P and Torres M 2013 The natural and social history of the indigenous lands and protected areas corridor of the Xingu River basin. Philos. Trans. R. Soc. Lond. B. Biol. Sci. 368 20120164

Wan Z, Zhang Y, Zhang Q and Li Z-L 2004 Quality assessment and validation of the MODIS global land surface temperature Int. J. Remote Sens. 25 261–74

Wang K, Wan Z, Wang P, Sparrow M, Liu J, Zhou X and Haginoya S 2005 Estimation of surface long wave radiation and broadband emissivity using Moderate Resolution Imaging Spectroradiometer (MODIS) land surface temperature/emissivity products J. Geophys. Res. 110 D11109

White M A, Thornton P E, Running S W and Nemani R R 2000 Parameterization and Sensitivity Analysis of the BIOME–BGC Terrestrial Ecosystem Model: Net Primary Production Controls Earth Interact. 4 1–85